



## **The intensity of the inflammatory response in experimental porcine bruises depends on time, anatomical location and sampling site**

**Barington, Kristiane; Skovgaard, Kerstin; Henriksen, Nicole Lind; Johansen, Anne Sofie Boyum; Jensen, Henrik Elvang**

*Published in:*  
Journal of Forensic and Legal Medicine

*Link to article, DOI:*  
[10.1016/j.jflm.2018.06.005](https://doi.org/10.1016/j.jflm.2018.06.005)

*Publication date:*  
2018

*Document Version*  
Peer reviewed version

[Link back to DTU Orbit](#)

*Citation (APA):*  
Barington, K., Skovgaard, K., Henriksen, N. L., Johansen, A. S. B., & Jensen, H. E. (2018). The intensity of the inflammatory response in experimental porcine bruises depends on time, anatomical location and sampling site. *Journal of Forensic and Legal Medicine*, 58, 130-139. <https://doi.org/10.1016/j.jflm.2018.06.005>

---

### **General rights**

Copyright and moral rights for the publications made accessible in the public portal are retained by the authors and/or other copyright owners and it is a condition of accessing publications that users recognise and abide by the legal requirements associated with these rights.

- Users may download and print one copy of any publication from the public portal for the purpose of private study or research.
- You may not further distribute the material or use it for any profit-making activity or commercial gain
- You may freely distribute the URL identifying the publication in the public portal

If you believe that this document breaches copyright please contact us providing details, and we will remove access to the work immediately and investigate your claim.

# Accepted Manuscript

The intensity of the inflammatory response in experimental porcine bruises depends on time, anatomical location and sampling site

Kristiane Barington, Kerstin Skovgaard, Nicole Lind Henriksen, Anne Sofie Boyum Johansen, Henrik Elvang Jensen



PII: S1752-928X(18)30119-7

DOI: [10.1016/j.jflm.2018.06.005](https://doi.org/10.1016/j.jflm.2018.06.005)

Reference: YJFLM 1689

To appear in: *Journal of Forensic and Legal Medicine*

Received Date: 12 March 2018

Revised Date: 24 May 2018

Accepted Date: 5 June 2018

Please cite this article as: Barington K, Skovgaard K, Henriksen NL, Boyum Johansen AS, Jensen HE, The intensity of the inflammatory response in experimental porcine bruises depends on time, anatomical location and sampling site, *Journal of Forensic and Legal Medicine* (2018), doi: 10.1016/j.jflm.2018.06.005.

This is a PDF file of an unedited manuscript that has been accepted for publication. As a service to our customers we are providing this early version of the manuscript. The manuscript will undergo copyediting, typesetting, and review of the resulting proof before it is published in its final form. Please note that during the production process errors may be discovered which could affect the content, and all legal disclaimers that apply to the journal pertain.

# **The intensity of the inflammatory response in experimental porcine bruises depends on time, anatomical location and sampling site**

Kristiane Barington<sup>1</sup>, Kerstin Skovgaard<sup>2</sup>, Nicole Lind Henriksen<sup>1</sup>, Anne Sofie Boyum Johansen<sup>1</sup>,  
Henrik Elvang Jensen<sup>1</sup>

<sup>1</sup> *Faculty of Health and Medical Sciences, University of Copenhagen, Ridebanevej 3, DK-1870  
Frederiksberg C, Denmark*

<sup>2</sup> *Department of Biotechnology and Biomedicine, Technical University of Denmark, Kemitorvet  
DK-2800 Kongens Lyngby, Denmark*

## **Corresponding author:**

Kristiane Barington

Faculty of Health and Medical Sciences, University of Copenhagen, Ridebanevej 3, DK-1870

Frederiksberg C, Denmark

E-mail: [krisb@sund.ku.dk](mailto:krisb@sund.ku.dk)

**Acknowledgements**

The authors wish to thank Karin Tarp at Section for Immunology and Vaccinology, National Veterinary Institute, Technical University of Denmark and Betina G. Andersen, Elizabeth W. Petersen, Frederik Andersen and Dennis Brok at Faculty of Health and Medical Sciences, University of Copenhagen Denmark for skilled technical and laboratory assistance.

**Declaration of interest**

None.

**Funding**

The study was funded by University of Copenhagen, Denmark. The funding source had no involvement in the experimental design, analysis and interpretation of the results.

**Ethical approval**

The experimental procedure was approved by the Danish Animal Inspectorate (2013–15–2934–00849) and were carried out in accordance with all institutional, and national guidelines.

**The intensity of the inflammatory response in experimental porcine bruises depends on time, anatomical location and sampling site**

## Abstract

The assessment of the age of bruises inflicted on livestock is an important component of veterinary forensic pathology investigations. However, the sampling site within a bruise, the anatomical location and the mass and speed of the object inflicting the blunt trauma might influence the intensity of the inflammatory reaction. In the present study, the variation of the inflammatory reaction within and along experimental porcine bruises was evaluated in order to determine the optimal sampling site. Moreover, we evaluated if a combination of histological characteristics and gene expression signatures was able to differentiate bruises according to anatomical location, age of bruises and the speed and mass of the object used to cause the impact.

Twelve experimental slaughter pigs were anesthetized, and on each animal four blunt traumas were inflicted on the back using either a plastic tube or an iron bar, respectively. The pigs were euthanized at 2, 5 or 8 h after infliction. Following gross examination, skin and underlying muscle tissue were sampled from the center and both ends of bruises and evaluated histologically. Subcutaneous fat tissue from the center of the bruises was sampled for quantitative real-time polymerase chain reaction to evaluate mRNA expression of 13 selected genes. Uninjured tissue was sampled from the right thigh of all pigs and served as control tissue.

The amount of tissue damage and the intensity of the inflammatory reaction in bruises depended on the sampling site within and along a bruise, the anatomical location and the age of the bruise. The optimal site for sampling, i.e. the most pronounced inflammatory reaction, was at the center of the bruises where the plastic tube or iron bar first struck the skin. Moreover, bruises inflicted in areas with a thin layer of subcutaneous fat tissue showed more damage and inflammation in the underlying muscle tissue compared to bruises inflicted in areas with a thicker layer of subcutaneous fat tissue. In addition, hemorrhage in the muscle tissue was more likely present when bruises were

inflicted with an iron bar compared to a plastic tube. Combining histology and mRNA expression of the 13 genes showed that the age of bruises could be determined with a precision of  $\pm 2.04$  h. Moreover, the age of bruises could be determined with a precision of  $\pm 1.84$  h based solely on mRNA expression of a selection of four genes.

**Keywords:** Time factors; Bruise; Forensic pathology; Gene expression signature; Animal model; Porcine; qPCR.

## Introduction

The assessment of the age of bruises inflicted on livestock is an important component of veterinary forensic pathology investigations.<sup>1,2</sup> Porcine bruises are predominantly inflicted within a timeframe of approximately 8 h prior to slaughter.<sup>1</sup> During this period, pigs are handled by several people during transport from the farm to the slaughterhouse.<sup>1</sup> Age assessment of bruises is carried out by veterinary pathologists and may in court be used to determine in whose custody the pig was at the time where the bruises were inflicted.

Several methods have been evaluated in humans and in animal models in order to obtain accurate age assessment of bruises.<sup>3-5</sup> Recently, a reproducible model for inflicting experimental bruises in pigs was developed and validated.<sup>6</sup> In the model, bruises with a tramline pattern, characterized by two parallel hemorrhages separated by apparently normal skin, were inflicted on the back of experimental pigs. Grossly and histologically, the lesions were comparable to forensic cases regarding bruises in slaughter pigs.<sup>1,6</sup> In the model, neutrophils and macrophages showed a time dependent response in skin and muscle tissue, and mRNA expression of 13 selected genes in subcutaneous fat tissue was able to determine the age of bruises with a precision of approximately  $\pm 2$  h.<sup>6,7</sup> Moreover, the histological characteristics and mRNA expression, apart from being time dependent, also reflected the force used to inflict the bruises.<sup>7,8</sup> In addition, the presence of hemorrhage in porcine skin and underlying muscle tissue depends on the speed and mass of the object causing the blunt trauma.<sup>9</sup> These studies were carried out in pigs with a body weight of 23 - 40 kg. However, in forensic cases of porcine bruises, the slaughter pigs have a body weight of approximately 100 kg. In slaughter pigs, the thicker layer of subcutaneous fat tissue may provide a higher degree of protection of the underlying muscle tissue compared to that of younger pigs. In addition, difference in age may affect the inflammatory response due to age-related alterations in the innate immune response.<sup>10,11</sup>



Forensic cases of porcine bruises typically involve pigs with several bruises located on the back.<sup>1</sup> In a previous study of pigs with multiple bruises, histological evaluation of two bruises from each animal resulted in a similar age estimate in 48% of the pigs due to variation in the inflammatory response between the bruises.<sup>12</sup> In addition, a higher degree of hemorrhage has been recorded in bruises inflicted near bones and in areas where the underlying muscle tissue is thin.<sup>9, 13</sup> Apart from the variation in the inflammatory reaction between bruises, variation may also occur within and along a bruise. This has been shown in rats, where the intensity of the inflammatory response was related to the proximity to the site of trauma.<sup>14</sup>

Therefore, the aim of the present study was to evaluate the amount of tissue damage and intensity of the inflammatory reaction within and along bruises in order to determine the optimal sampling site for forensic evaluation. Moreover, we evaluated if a combination of histological characteristics and a gene expression signature of 13 selected genes was able to differentiate bruises according to anatomical location, age of the bruises and the object (mass and speed) used for inflicting the bruises.

## Methods

### *Animals*

In total, 12 specific pathogen-free, female, Yorkshire-Landrace crossbred pigs with a mean body weight of 100 kg (91-115 kg) were used. All pigs were acclimatized for one week and housed individually before entering the experiment. They were fed a commercial pig diet twice a day and had free access to tap water. All animals remained healthy during the period of acclimatization.

### *Experimental procedure*

The experimental procedure was approved by the Danish Animal Inspectorate (2013–15–2934–00849). All pigs were anesthetized using the same protocol as recently described.<sup>6</sup> During a period of 3 to 4 min four blunt traumas (area of impact Nos. 1, 2, 3 and 4) were inflicted on the back along the right *M. longissimus dorsi* from the area caudal to the scapula to the lumbar region of each pig using a plastic tube or an iron bar (Table 1, Fig. 1). The blunt traumas were inflicted with a force of 6.52 N/mm<sup>2</sup> using a mechanical device and procedure described recently.<sup>6</sup> The mechanical device consisted of a spring fixed in a rotatable wheel to which a plastic tube or an iron bar could be attached.<sup>6</sup> Regardless of the object (plastic tube and iron bar) the wheel was turned 180° and the same amount of kinetic energy was transferred to the area of impact. Following infliction of trauma, pigs were left in anesthesia for 2, 5 and 8 h (Table 1), and thereafter euthanized by an overdose of pentobarbital given intravenously (Glostrup Apotek, Glostrup, Denmark).

### *Speed at impact*

Measurements of the speed of the plastic tube and the iron bar were carried out at the Danish Technological Institute (Taastrup, Denmark). A high-speed camera (LQ-201CL, JAI) was equipped with a LINOS Inspec.x M lens, giving a calibrated pixel size of 0.000655 m at a 1.2 m focal

distance. The JAI line camera gave a time resolution of 1/30.000 s and a (1D)-spatial resolution of 0.000665 m of the impact zone. The recorded images gave a sampled version of the tube position during impact (displayed as a relatively straight line at an angle =  $\alpha$ ). Based on this the impact speed was calculated as  $V = (0.000655 \text{ m} \times 30000 \text{ s}^{-1}) / \tan(\alpha)$ .

### *Kinetic energy*

The amount of kinetic energy transferred to the area of impact was calculated from the impact speed (Supplementary material 1).

### *Gross pathology*

During the first hour after infliction and post-mortem, each pig was subjected to gross evaluation of each of the four areas of impact. Post-mortem, the pattern of bruises seen from the skin surface was classified as tramline (two parallel lines of hemorrhage) or fused (a single line of hemorrhage).

Moreover, the dimensions and distances between bruises were recorded and the affected skin areas were cut out *in toto* including the underlying part of *M. longissimus dorsi*. Each bruise was cross-sectioned in slices of 0.5 to 1 cm, and the presence of hemorrhage in the subcutaneous fat tissue and muscle tissue was recorded. Finally, all pigs were subjected to a total necropsy.<sup>15</sup>

### *Histology*

From each of the areas of impact (Nos. 1-4), 5 slices of skin and muscle tissue were sampled from the center (B, n=3), the dorsal end (A, n=1) and the ventral end (C, n=1) of the bruises (Fig. 2). In addition, uninjured skin and muscle tissue were sampled from the right thigh of each pig and served as control tissue. For histology, the samples were treated as described previously before tissue sections were cut and stained with hematoxylin and eosin.<sup>6, 16</sup> All sections were blinded and evaluated by a single observer. However, 53 out of 240 tissue sections were randomly selected and

evaluated by a second observer. Cohen's kappa or Cohens weighted kappa were calculated on each of the histological variables (see Table 15 in Ref [17].

Neutrophils and macrophages were scored on a semiquantitative scale: (0) Absence of neutrophils or macrophages, respectively (1) 1-10 neutrophils or macrophages, respectively (2) 11-30 neutrophils or macrophages, respectively (3) >30 neutrophils or macrophages, respectively. The scoring was carried out in the dermis, subcutaneous fat and muscle tissue in a high power field (400 fold magnification) in the area with the highest density of macrophages and neutrophils. In the dermis and muscle tissue, hemorrhage was registered as present or absent. In the subcutis, the density of hemorrhage was registered as the percentile area of extravasated erythrocytes in a low power field (100 fold magnification) and scored either as (0) absent, (1) minor: <12.5%, (2) moderate: 12.5-25%, (3) severe >25%. In the muscle tissue, the percentile area of necrosis was evaluated in the area with the highest density of necrotic muscle fibers and scored according to the following scale in a low power field (100 fold magnification): (0) No necrosis: absence of necrotic muscle fibers, (1) minor necrosis: <12.5%, (2) moderate necrosis: 12.5-50%, (3) severe necrosis: >50%.<sup>6</sup>

In addition, the thickness of the subcutaneous tissue was measured with a caliper at the center of the tissue sections.

#### *qPCR*

From the center (B) of all areas of impact (Nos. 1-4), subcutaneous fat tissue (0.5 cm x 0.5 cm x 0.5 cm) was sampled and preserved in 4.5 mL of RNAlater, that was cooled at 5°C for 24 h and then stored at -20 °C until extraction. In addition, uninjured subcutaneous fat tissue was sampled from the thighs of the pigs and treated similarly. Extraction, quantitation and quality assessment of RNA were carried out as recently described.<sup>7</sup> RNA integrity numbers were between 6.7 and 9.2 (average:

8.3). RNA was stored at -80 °C until converted into cDNA. From each sample, duplicate cDNA syntheses were made.<sup>7</sup> Primers were synthesized at Sigma Aldrich. Pre-amplification and quantitative real time polymerase chain reaction (qPCR) was performed to evaluate mRNA expression of the 13 genes of interest and the 6 reference genes listed in Table 2. In a recent study of experimental bruises in pigs, a time dependent expression pattern was observed for the 13 genes of interest.<sup>7</sup> qPCR of the preamplified cDNA was performed in a 192.24 Dynamic Array (Fluidigm, San Francisco, CA, USA) combining 192 preamplified samples with 24 primer sets in 4608 individual and simultaneous qPCR reactions. Thorough descriptions of preamplification and qPCR have recently been described.<sup>7</sup>

#### *Data analysis and statistics*

##### *Gross data*

Logistic regression for repeated measures (Generalized estimating equations for binary data with logit link function) were applied to evaluate if bruises inflicted with either a plastic tube or an iron bar differed with regards to pattern (tramline or fused) and presence of gross hemorrhage in the underlying muscle tissue (SAS Enterprise Guide 7.1). Mean and standard deviations (SD) were calculated on the dimensions and distances between bruises measured on the surface of the skin. The thickness of the subcutaneous tissue in the four areas of impact was compared by a two way ANOVA (SAS Enterprise Guide 7.1).

##### *Histology data*

To evaluate the variation between the ends (sampling site A and C) and the center (sampling site B) of the bruises, the histological data were autoscaled by multiplication with the inverse standard before principal component analysis (PCA) in LatentX 2.13 (Frederiksberg, Denmark). The result of the PCA was presented in two plots describing scores and loadings, respectively. PCA scores

were used to determine any grouping of the data according to sampling sites (A, B and C). PCA loadings were used to determine how histological variables influenced the PCA scores. Information on how to interpret PCA scores and loadings is presented elsewhere.<sup>18</sup> Additional descriptive statistics are presented in Ref [17]. Moreover, differences (odds ratios) in single histological variables between the objects (plastic tube or iron bar), sampling site, anatomical location and bruise age are presented in Ref [17].

#### *mRNA expression data*

Pre-processing data: To compensate for variation between dynamic chips three highly stable samples were used as interplate calibrators. Then, the data were corrected for PCR efficiency for each primer. GeNorm and GeNormFinder were used to identify the most stable reference genes (B2M, HPRT1, PPIA) and the geometric mean of these was used to normalize all data for each cDNA replicate in GenEx5 (MultiD Analyses AB Sweden).<sup>19, 20</sup> The technical repeats of cDNA were compared and excluded if the deviation was more than 1.5 Cq for more than 15% of the samples. The average of the technical repeats of cDNA was calculated and the Cq values were transformed to a linear scale (relative quantities) and log<sub>2</sub> transformed.<sup>7</sup>

For each pig, the average gene expression (relative quantities) within the bruises was calculated. These values were used to calculate the average expression for each bruise age (2, 5 and 8 h) and finally, the relative expression of genes in bruises aged 2, 5 and 8 h was calculated relatively to the average expression in the control tissue.

#### *Combination of data from histology and mRNA expression*

Regardless of the sampling site (ends (A and C) or center (B)) of the bruise the maximum scores for each of the histological parameters were registered for each of the bruises. Then gene expression data (log<sub>2</sub> transformed values) and histology data were combined and autoscaled by multiplication

with the inverse standard error before PCA and partial least squares regression (PLS) were done in LatentiX 2.13 (Frederiksberg, Denmark). First, a PCA including all bruises and control tissues was made and plots of scores and loading were evaluated. Then, control tissues were excluded and a new PCA was calculated to describe if histology and gene expression data could differentiate bruises according to the anatomical location (area of impact Nos. 1 to 4) and the age (2h, 5h and 8h). The results from these PCAs were presented in two plots describing scores and loadings. PCA scores were used to determine any grouping of the data according to anatomical location and age. PCA loadings were used to determine how the histological variables and gene expression variables influenced the PCA scores.<sup>18</sup>

On the same data, PLS with full cross validation was carried out in order to obtain a model to predict the age of bruises based on histology and mRNA expression data. In addition, a PCA and a PLS with full cross validation was carried out on the mRNA expression data of the four most important genes for determining bruise age, i.e. the four genes with the highest negative or positive regression coefficients (SELE, SELP, IL6, NFKB1). The result from the PCA was presented as a score plot in order to visualize grouping according to age.

## Results

### *Speed at impact and kinetic energy*

The speeds at impact of the objects (plastic tube and iron bar) are presented in Table 1. The kinetic energy transferred to the area of impact was 26 J for both objects.

### *Gross pathology*

In total, 48 bruises were inflicted on the 12 pigs using a plastic tube or an iron bar. During the first 3 minutes, all bruises developed in a similar pattern regardless of the object. Within the first 20-30 sec two symmetrical, convex red lines (connected in both ends) became visible on the skin surface.

After 2-3 min the distance between the red lines decreased before they almost fused. From 15 to 60 min after infliction, the skin either appeared normal or a vague redness was visible in the areas. The appearance of the lesions did not change during the rest of the experimental period (2 to 8 h) (Fig. 1).

Gross evaluations carried out post mortem are presented in Table 3. If visible on the skin surface, the pattern of bruises could be characterized as tramlines or as fused. Tramline bruises were characterized by two parallel lines of redness separated by apparently normal skin. Fused bruises were characterized by a single line of redness. On cross sections, two areas of hemorrhage separated by apparently normal fat tissue were present in the subcutaneous tissue in the center of 46 out of the 48 bruises (Fig. 1, Table 3).

### *Histology*

Variation within and along the bruises:

In total, 240 tissue sections from the 48 bruises were evaluated. To some extent the inflammatory response differed according to the sampling sites (A, B and C). The differentiation was seen along principal component nos. 1 and 2 (Fig. 3). Based on the loadings (Fig. 4) and odds ratios (see Table 6 in Ref [17], samples from the center (B) of the bruises were generally characterized by higher scores in all histological parameters compared to samples from the ventral end of the bruise (C). A large variation was seen in the samples from the dorsal end (A) (Fig. 3). The raw data were presented in Supplementary material 2.



### *Combination of data from histology and mRNA expression*

Data consisted of bruises inflicted with a plastic tube (n=24) or an iron bar (n=23) and control tissue from the thighs of the pigs (n=11). A single bruise (8 h, iron bar, area of impact No. 1) and a control sample were excluded due to missing mRNA-expression data (Supplementary material 3).

### *Mass and speed*

Bruises clearly differed from the control tissue. However, no grouping according to the object, i.e. plastic tube or iron bar, was found in the PCA plot. However, when looking at single histological variables hemorrhage together with high neutrophil score in the muscle tissue were more likely to be present if bruises were inflicted using an iron bar compared to a plastic tube (see Table 7 in Ref [17]). Moreover, a high neutrophil score in the dermis was more likely if bruises were inflicted using a plastic tube compared to an iron bar (see Table 7 in Ref [17]).

### *Anatomical location of the bruise*

Bruises tended to group according to the anatomical location (area of impact Nos. 1 and 2 vs. 3 and 4) along principal component no. 2 (Fig. 5). Based on the loadings, bruises inflicted in area of impact Nos. 3 and 4 had higher scores in the histological parameters in the subcutaneous fat tissue and muscle tissue compared to bruises inflicted in area Nos. 1 and 2 (Fig 6). Especially, muscle parameters (neutrophils and macrophages, hemorrhage and necrosis) were high in bruises in area Nos. 3 and 4 (Fig 6) (see Table 13 in Ref [17]). Gene expression data contributed less to the grouping of bruises at the four anatomical locations.

### *Age of bruises*

Grouping of bruises aged 2, 5 and 8 h was seen along the first principal component (Fig. 8). This was mainly explained by the gene expression variables while the histology variables contributed less (Fig 9) (See Table 14 in Ref [17]. PLS including all bruises (plastic tube, iron bar, all ages and areas of impact) and variables was able to predict the age of bruises with a root mean square error of 1.02 h, meaning that in 95% of bruises, the model was able to predict the age with a precision of  $\pm 2.04$  h. The model had a standard error of precision of 1.03, a bias of -0.05 and a correlation coefficient of 0.82. In the second PLS-component the explained variance in Y and X was 83% and 42%, respectively. Regression coefficients for all variables in the second PLS-component are presented in Table 4. The mRNA expression of SELP, NFKB1, IL6 and SELE all had regression coefficients below -0.15 meaning that the mRNA expression was upregulated at first and then declined during the following 8 h after infliction. Based on these four genes, a more distinct grouping of bruises according to age was seen (Fig. 10). A PLS including the four genes was able to predict the age of bruises with a root mean square error of 0.92 h, meaning that in 95% of bruises, the model was able to predict the age with a precision of  $\pm 1.84$  h. The model had a standard error of precision of 0.93, a bias of 0.002 and a correlation coefficient of 0.86. In the first PLS-component the explained variance in Y and X was 87% and 83%, respectively.

In Table 5, the mean gene expression in the bruises, relative to the mean expression in the control tissue scaled to one is presented.

#### *Thickness of the subcutaneous fat tissue*

The thickness of the subcutaneous fat tissue was normally distributed and differed significantly between the four areas of impact ( $P < 0.0001$ ), (Fig. 11).

## Discussion

The amount of tissue damage and the intensity of the inflammatory reaction in bruises depended on the sampling site within a single bruise, the anatomical location and the age of the bruise.

Combining histology and mRNA expression of 13 selected genes, the age of bruises could be determined with a precision of  $\pm 2.04$  h. Moreover, the gene expression of SELE, SELP, IL6 and NFKB1 was even able to determine the age of bruises with a precision of  $\pm 1.84$  h.

Grossly, bruises inflicted with a plastic tube and an iron bar differed with respect to the pattern of bruises on the skin surface and the presence of hemorrhage in the muscle tissue. However, these differences were not statistically significant. Histologically, the odds for muscle hemorrhage in bruises inflicted by an iron bar were 5 times the odds for muscle hemorrhage in bruises inflicted with a plastic tube. In addition, the odds for high neutrophil infiltration in the dermis were 5 times the odds for high neutrophil infiltration in the muscle tissue (see Table 7 in Ref [17]). The gene expression profile was not able to differentiate between bruises inflicted with a plastic tube and an iron bar. The light weight plastic tube reached a impact speed of more than twice of the heavier iron bar (Table 1). However the energy transferred from the spring in the mechanical device to the area of impact was the same regardless of the object (plastic tube or iron bar). In another porcine bruise model, objects with high speed (104 m/second) and low weight (3.15 g) caused hemorrhage in the upper skin layers, while heavier (2.5 kg) objects with low speed (4m/second) caused deep hemorrhage in the muscle tissue even though the kinetic energy per area was comparable.<sup>9</sup>

At gross inspection, hemorrhage in the muscle tissue was recognized in 21% and 46% of bruises inflicted with a plastic tube and an iron bar, respectively. In comparison, hemorrhage was grossly visible in 57.5% of bruises in pigs weighing 30 kg.<sup>6</sup> These differences between small and large pigs could be due to differences in the volume and maturation of supporting tissue that overlies the

vessels, amount of fibrous tissue and differences in the density of vessels, all of which changes during growth.<sup>21</sup>

Histologically, the intensity of the inflammatory reaction and the amount of hemorrhage and necrosis were often most pronounced in samples from the center of the bruises, less pronounced in samples from the ventral end, and variable at the dorsal end. As the shape of the area of impact was convex, the plastic tube or iron bar struck at the central part of the bruise at first and, therefore, transferred most of the energy into this part resulting in more tissue damage compared to the two ends of the bruises. Similarly, injection of blood into rodent skin showed that the intensity of the inflammatory response was directly related to the proximity to the site of trauma, and it was found that areas containing blood that had diffused from the site of trauma, showed a low grade of inflammatory reaction.<sup>14</sup> Generally, bruises inflicted in area Nos. 3 and 4 showed a higher degree of hemorrhage, necrosis, and infiltration of neutrophils and macrophages in the muscle tissue compared to bruises in area Nos. 1 and 2. This difference could be explained by the presence of a thinner layer of subcutaneous tissue at area Nos. 3 and 4, which means that a higher amount of energy probably was transferred to the underlying muscle tissue causing more damage. In other porcine and avian models, tissue damage has also been found to depend on the anatomical location of the bruises, and more tissue damage has been observed in bruises inflicted near bones and in areas with a thin layer of muscle tissue.<sup>9, 13</sup> However, the difference between bruises in area Nos. 1 and 2 versus areas Nos. 3 and 4 may also partly be due to the difference in time (minutes), during which these were inflicted. In comparison, in rabbits and chickens, infliction of multiple bruises have been shown to affect how fast the lesions heal.<sup>22, 23</sup> Possibly, the vasodilation, hyperemia and release of inflammatory mediators after infliction of the first bruise could intensify the inflammation and tissue damage in the subsequent bruises.

Mathematical age prediction models based on experimental data could potentially be used in a forensic setting.<sup>7</sup> Combining data on bruises of unknown age and data from the experimental bruises, the age of the unknown bruises could be determined by applying a partial least squares regression analysis. Based on histology and gene expression, the age of bruises could be predicted with a precision of  $\pm 2.04$  h. This is in complete accordance to a previous study in pigs weighing approximately 30 kg.<sup>7</sup> Several of the genes (IL6, NFKB1, SELE, PTGS2, CCL2, ICAM1, FOS, TNFAIP3 and SELP) were upregulated in bruises being 2 h old and then decreased with increasing age of the bruise. The same pattern of gene regulation was present in bruises in pigs weighing 30 kg although at higher fold change differences.<sup>7</sup> This difference between small and large pigs could be due to differences in thickness of the subcutaneous fat tissue or age-related alterations of the inflammatory gene expression response to blunt trauma.<sup>10</sup>

The mRNA expression profile of four genes centrally involved in inflammation, (the cell adhesion molecules SELE and SELP, the proinflammatory cytokine IL6 and the transcription factor NFKB1) were able to predict the age of bruises with a precision of  $\pm 1.84$  h. The model had a lower standard error of precision, a smaller bias and a higher correlation coefficient and higher explained variance in X and Y compared to the PLS based on a combination of histology and gene expression data. This imply that the estimation of the age of bruises is more precise if based on a gene expression profile alone than by the combination of gene expression and histology. Part of the difference in the precision is caused by “noise” from the histological and gene expression variables less important for estimating the age, i.e. variables with regression coefficients close to zero (Table 5). However, the grouping of bruises by age was mostly explained by the mRNA expression variables and less by the histological variables. In experimental bruises in pigs weighing 30 kg, neutrophils in the subcutaneous tissue and macrophages in the muscle tissue showed a time dependent increase.<sup>6</sup> Studies of bruises in humans have also demonstrated variability in timing and sequence of

inflammatory changes when evaluated histologically.<sup>4, 24</sup> The lack of a clear time dependency in the histological parameters in the present study might be explained by a high degree of animal to animal variation. It could be speculated that mRNA expression is less affected by the variation between pigs. Moreover, studies have shown that mRNA expression does not necessarily correlate with the amount of protein synthesized due to post-transcriptional mechanisms involved in turning the mRNA into protein.<sup>25</sup>

## Conclusions

The intensity of the inflammatory reaction in bruises depended on the sampling site within the bruise, the anatomical location and the age of the bruise. The most pronounced inflammatory reaction together with hemorrhage and muscle fiber necrosis were found in samples from the center of the bruises, i.e. at the site where the plastic tube or iron bar first struck the skin. Therefore, this is the optimal site for sampling. Moreover, bruises inflicted in areas with a thin layer of subcutaneous fat tissue revealed more damage and inflammation in the underlying muscle tissue compared to bruises inflicted in areas with a thicker layer of subcutaneous fat tissue. In addition, hemorrhage in the muscle tissue was more likely present when bruises were inflicted with an iron bar compared to a plastic tube. Combining histology and mRNA expression of 13 genes showed that the age of bruises could be determined with a precision of  $\pm 2.04$  h. Moreover, the age of bruises could be determined with a precision of  $\pm 1.84$  h based on mRNA expression of a selection of four genes only.

## References

1. Barington K, Jensen HE. Forensic cases of bruises in pigs. *Vet Rec.* 2013;173:526-530.
2. Ressel L, Hetzel U, Ricci E. Blunt force trauma in veterinary forensic pathology. *Vet Pathol.* 2016;53:941-961.
3. Barington K, Jensen HE. Experimental animal models of bruises in forensic medicine – a review. *Scand J Lab Anim Sci.* 2015;41:14.
4. Byard RW, Wick R, Gilbert JD, Donald T. Histological dating of moribund infants and young children. *Forensic Sci Med Pathol.* 2008;4:187-192.
5. Hughes VK, Ellis PS, Langlois NEI. Alternative light source (polilight) illumination with digital image analysis does not assist in determining the age of bruises. *Forensic Sci Int.* 2006;158:104-107.
6. Barington K, Jensen HE. A novel, comprehensive and reproducible porcine model for the timing of bruises in forensic pathology. *Forensic Sci Med Pathol.* 2016;12:58-67.
7. Barington K, Jensen HE, Skovgaard K. Forensic aspects of gene expression signatures for age determination in bruises as evaluated in an experimental porcine model. *Forensic Sci Med Pathol.* 2017;13:151-160.
8. Barington K, Jensen HE. The impact of force on the timing of bruises evaluated in a porcine model. *J Forensic Leg Med.* 2016;40:61-66.

9. Randerberg LL, Winnem AM, Langlois NE, Larsen ELP, Haaverstad R, Skallerud B, Haugen OA, Svaasand LO. Skin changes following minor trauma. *Lasers Surg Med.* 2007;39:403-413.
10. Gruver AL, Hudson LL, Sempowski GD. Immunosenescence of ageing. *J Pathol.* 2007;211:144-156.
11. Sgonc R, Gruber J. Age-related aspects of cutaneous wound healing: A mini-review. *Gerontology.* 2013;59: 159-164.
12. Barington K, Agger JFG, Nielsen SS, Dich-Jørgensen K, Jensen HE. Gross and histopathological evaluation of human inflicted bruises in Danish slaughter pigs. *BMC Vet Res.* 2016;12:247.
13. Hamdy MK, May KN, Powers JJ. Some physical and physiological factors affecting poultry bruises. *Poult Sci.* 1961;40:790-795.
14. Ross C, Byard RW, Langlois NEI. Does the intensity of the inflammatory reaction in a bruise depend on the proximity to the site of trauma. *Forensic Sci Med Pathol.* 2013;9:358-362.
15. Madsen LW, Jensen HE. Necropsy of the pig. In: Jensen HE, editor. *Necropsy. A handbook and atlas*, Denmark: Biofolia; 2011, p. 83-134.
16. Grizzle WE, Fredenburgh JL, Myers RB, Billings PE, Spencer LT, Bancroft JD et al. Chapter 4-9. In: Bancroft JD, Gamble M, editors. *Theory and practice of histological techniques*. 6th ed, Philadelphia: Churchill Livingstone Elsevier; 2008, p. 53-134.
17. Barington K, Skovgaard K, Henriksen NL, Johansen ASB, Jensen HE. Histological evaluation of experimental porcine bruises. *J Forensic Leg Med, Data in Brief. Submitted.*
18. Bro R, Smilde AK. Principal component analysis. *Anal Methods.* 2014;6:2812-2831.
19. Vandesompele J, De Preter K, Pattyn F, Poppe B, Van Roy N, De Paepe A, Speleman F. Accurate normalization of real-time quantitative RT-PCR data by geometric averaging of multiple internal control genes. *Genome Biol.* 2002;3:research0034.



20. Andersen CL, Jensen JL, Ørntoft TF. Normalization of real-time quantitative reverse transcription-PCR data: a model-based variance estimation approach to identify genes suited for normalization, applied to bladder and colon cancer data sets. *Cancer Res.* 2004;64:5245–5250.
21. Saukko P, Knight B. Knight's Forensic Pathology. 4<sup>th</sup> ed. Boca Ranton, Florida: CRC Press; 2016.
22. Hamdy M, Kunkle L, Rheins M, Deatherage F. Bruised tissue 3. Some factors affecting experimental bruises. *J Anim Sci.* 1957;16:496-501.
23. Hamdy M, May K, Powers J. Some physiological factors affecting poultry bruises. *Poult Sci.* 1961;40:790-795.
24. Ross CG, Langlois NEI, Heath K, Byard W. Further evidence for a lack of reliability in the histologic ageing of bruises – an autopsy study. *Aust J Forensic Sci.* 2015;47:224-229.
25. Maier T, Güell M, Serrano L. Correlation of mRNA and protein in complex biological samples. *FEBS Lett.* 2009;583:3966-3973.

### Figure legends

**Figure 1:** Bruises on pig skin inflicted with an iron bar. Bruises were located on the back in area of impact Nos. 1 to 4. Inset: Cross section of a bruise. Hemorrhage is seen in the subcutaneous fat tissue and the underlying muscle tissue.

**Figure 2:** Sampling of bruises for histology. From each bruise, 5 slices of skin and underlying muscle tissue were sampled from the center (B, n=3) and the dorsal (A, n=1) and ventral ends (C, n=1) of the bruises.

**Figure 3:** Principal component analysis (PCA) scores based on histological data from sampling site A (blue), B (red) and C (green) in all bruises. Each square represents a tissue sample consisting of skin and muscle tissue. The percentages placed in brackets denote the variation in the data explained in principal component 1(PC#1) and principal component 2 (PC#2). A tendency for grouping of samples according to sampling site is seen. Samples from the ventral end (C) are mainly located in the lower left quadrant and samples from the center (B) are located in the two upper quadrants and in the lower right quadrant. Samples from the dorsal end (A) are scattered in all four quadrants.

**Figure 4:** Loadings from the principal component analysis (Fig. 3) based on histological data from sampling site A, B and C from all bruises. The percentages placed in brackets denote the variation in the data explained in principal component 1(PC#1) and principal component 2 (PC#2). The histological variables are located in the upper and lower right quadrant, i.e., samples from the center (B) are generally characterized by higher scores in the histological parameters compared to samples from the ventral end (C).

**Fig 5:** Principal component analysis (PCA) scores based on histological and gene expression data from all bruises. Bruises tend to group according to the anatomical location: Area of impact No. 1 (yellow), area of impact No. 2 (green), area of impact N. 3 (blue), and area of impact No. 4 (red). The percentages placed in brackets denote the variation in the data explained in principal component 1(PC#1) and principal component 2 (PC#2).

**Figure 6:** Loadings from principal component analysis (Fig. 5) based on histological and gene expression data from all bruises. The percentages placed in brackets denote the variation in the data explained in principal component 1(PC#1) and principal component 2 (PC#2). Neutrophils, macrophages, hemorrhage and necrosis in the muscle tissue were more pronounced in bruises inflicted in area Nos. 3 and 4 compared to area Nos. 1 and 2. Neutrophils in the dermis and the mRNA expression of CCL2, SELP, FOS, SELE, IL6, PTGS2 and NFKB1 did not contribute to the grouping according to anatomical location as their loadings were close to zero on PC#2. The remaining variables contributed to variable extend to the grouping according to anatomical location.

**Fig 7:** Porcine muscle tissue underlying a bruise inflicted with a plastic tube (5 h old, sampled from the center, area of impact No. 4). Neutrophils and macrophages have infiltrated the necrotic muscle fibers and hemorrhage is present in the interstitial space. Bar 100µm.

**Fig 8:** Principal component analysis (PCA) scores based on histological and gene expression data from all bruises. The percentages placed in brackets denote the variation in the data explained in principal component 1 (PC#1) and principal component 2 (PC#2). Bruises tended to group according to age: 2 h (blue), 5 h (green), 8 h (red), along PC#1.

**Figure 9:** Loadings from principal component analysis (Fig. 8) based on histological and gene expression data from all bruises. The percentages placed in brackets denote the variation in the data explained in principal component 1(PC#1) and principal component 2 (PC#2). For interpretation of loadings the score plot in Figure 7 was used. Especially gene expression variables contributed to the grouping according to bruise age. Genes were upregulated in bruises being 2 h old and then decreased with increasing age of the bruise. The histological variables contributed less to the grouping according to age as their loadings were close to zero along PC#1.

**Fig 10:** Principal component analysis (PCA) scores based on the gene expression of IL6, NFKB1, SELE and SELP in all bruises. Bruises grouped according to age: 2 h (blue), 5 h (green), 8 h (red). The percentages placed in brackets denote the variation in the data explained in principal component 1(PC#1) and principal component 2 (PC#2).

**Fig. 11:** The mean thickness and standard deviation of the subcutaneous fat tissue (mm) at each of the four areas of impact. The mean thickness of the subcutaneous tissue decreased from area of impact Nos. 1 to 4.

**Supplementary material**

**Supplementary material 1:** Calculation of the kinetic energy transferred to the area of impact. **Supplementary material 2:** Histology data from evaluation of a total of 240 tissue sections (A, B and C samples).

**Supplementary material 3:** Histology data (maximum values) and mRNA expression data (log<sub>2</sub> transformed values) for bruises and control tissue.

**Table 1:** Summary of the number of pigs, the age of bruises and the object used to inflict bruises including the mass and the speed of the objects at impact. Four bruises were inflicted on each pig using either a plastic tube or an iron bar, and four pigs were euthanized at each time point (2, 5 and 8 h). The plastic tube was attached to an adapter (0.146 kg) that was inserted into the mechanical device.<sup>6</sup> The iron bar was attached directly to the mechanical device.

No. of pigs	Bruise age (h)	Object	Mass (kg)	Speed (m/s)
6	2, 5 or 8	Plastic tube	0.047	47.4
6	2, 5 or 8	Iron bar	0.400	19.7

**Table 2:**

ACCEPTED MANUSCRIPT

**Table 2:** Gene symbol, gene name and sequences of forward (F) and reverse (R) primers.

Gene symbol	Gene name	Sequence (5' to 3')
APOA1	Apolipoprotein A-I	F:GTTCTGGGACAACCTGGAAA R: GCTGCACCTTCTTCTTCACC
CCL2	Chemokine (C-C Motif) Ligand 2	F:CTTCTGCACCCAGGTCCTT R: CGCTGCATCGAGATCTTCTT
CFD	Complement Factor D	F:CCTCGGAGCAGCTGTATGT R: ATGCCATGTAGGGTCTCTCG
FOS	FBJ Murine Osteosarcoma Viral Oncogene Homolog	F:CTCCAAGCGGAGACAGACC R: CTTCTCCTTCAGCAGGTTGG
ICAM1	Intercellular Adhesion Molecule 1	F:AAGCTTCTCCTGCTCTGCTG R: GGGGTCCATACAGGACACTG
IFNA1	Interferon Alpha 1	F:ATCGTCAGGGCAGAAGTCAT R: CAGGTGTCTGTCACTCCTTC
IL6	Interleukin 6	F: TGGGTTCAATCAGGAGACCT R: CAGCCTCGACATTTCCCTTA
NFKB1	Nuclear Factor Of Kappa Light Polypeptide Gene Enhancer In B-Cells 1	F:CTCGCACAAGGAGACATGAA R: GGGTAGCCCAGTTTTTGTCA
PLAT	Plasminogen Activator, Tissue	F:TGCTTCCAGGAGAGGTTCC R: CTCTCCAGGGACCAGCCTAT
PTGS2	Prostaglandin-Endo-peroxide Synthase 2	F:GAACTTACAGGAGAGAAGGAAATGG R: TTTCTACCAGAAGGGCAGGA



SELE	Selectin E	F:GGATGCTGCCTACTTGTGAAG R: CAGGAGCCAGAGGAGAAATG
SELP	Selectin P	F:CCTAGCAGGGCCATTGAC R: CCCACCCATCACTAAACCTG
TNFAIP3	Tumor Necrosis Factor, Alpha- Induced Protein 3	F:CCCAGCTTTCTCTCATGGAC R: TTGGTTCTTCTGCCGTCTCT
ACTB	Actin, Beta	F: CTACGTCGCCCTGGACTTC R: GCAGCTCGTAGCTCTTCTCC
B2M	Beta-2-Microglobulin	F: TGAAGCACGTGACTCTCGAT R: CTCTGTGATGCCGGTTAGTG
HPRT1	Hypoxanthine phosphoribosyl- transferase I	F: ACACTGGCAAAACAATGCAA R: TGCAACCTTGACCATCTTTG
PPIA	Peptidylprolyl isomerase A (cyclophilin A)	F: CAAGACTGAGTGGTTGGATGG R: TGTCCACAGTCAGCAATGGT
RPL13A	Ribosomal protein L13a	F: ATTGTGGCCAAGCAGGTACT R: AATTGCCAGAAATGTTGATGC
TBP	TATA box binding protein	F: ACGTTCGGTTTAGGTTGCAG R: CAGGAACGCTCTGGAGTTCT

**Table 3:** Post-mortem, gross evaluation of the areas of impact seen on the skin surface and on cross section. No significant difference were seen in bruise pattern ( $p=0.19$ ) or presence of hemorrhage in the muscle tissue ( $p=0.12$ ) between bruises inflicted with a plastic tube and an iron bar.

Gross pathology	Plastic tube	Iron bar
<u>Skin surface</u>		
Number of visible bruises	24 of 24 (100 %)	22 of 24 (92%)
Mean length $\pm$ SD of bruises	$8 \pm 2.5$ cm	$7 \pm 1.3$ cm
Mean distance $\pm$ SD between bruises	$7 \pm 1.3$ cm	$7 \pm 0.8$ cm
Number of bruises with tram line pattern	20 of 24 (83%)	11 of 22 (50%)
Mean width $\pm$ SD of each of the hemorrhages	$0.3 \pm 0.3$ cm	$0.2 \pm 0.1$ cm
Mean distance $\pm$ SD between the hemorrhages	$0.2 \pm 0.1$ cm	$0.2 \pm 0.1$ cm
Number of bruises with fused pattern	4 of 24 (8%)	11 of 22 (50%)
Mean width $\pm$ SD of hemorrhage	$1 \pm 0.3$ cm	$0.8 \pm 0.1$ cm
<u>Cross section</u>		
Areas of impact with hemorrhage in subcutis	24 of 24 (100%)	24 of 24 (100%)
Areas of impact with hemorrhage in muscle tissue	5 of 24 (21%)	11 of 24 (46%)

**Table 4:** Regression coefficients for a PLS-model for prediction of bruise age based on histology and gene expression data.

Variable	Regression coefficients
Selectin P	-0.19
Nuclear Factor Of Kappa Light Poly-peptide Gene Enhancer In B-Cells 1	-0.18

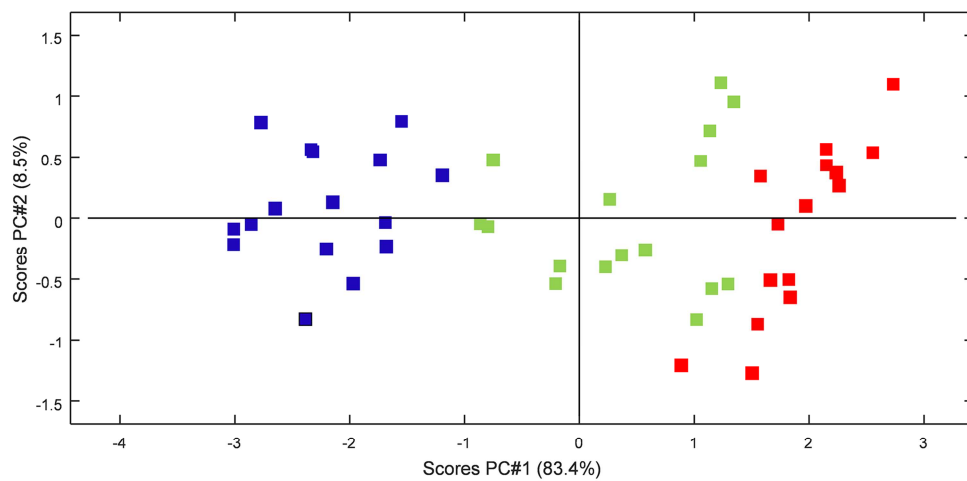
---

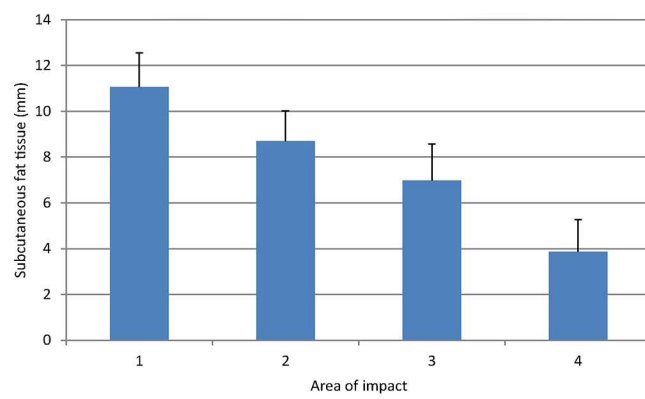
Interleukin 6	-0.18
Selectin E	-0.16
Tumor Necrosis Factor, Alpha-Induced Protein 3	0.14
Intercellular Adhesion Molecule 1	-0.11
Chemokine (C-C Motif) Ligand 2	-0.11
Prostaglandin-Endo-peroxide Synthase 2	-0.08
Macrophages in the muscle tissue	0.08
Hemorrhage in the dermis	0.07
Neutrophils in the subcutaneous tissue	-0.07
FBJ Murine Osteosarcoma Viral Oncogene Homolog	-0.06
Neutrophils in the muscle tissue	0.06
Plasminogen Activator, Tissue	-0.05
Hemorrhage in the muscle tissue	0.04
Hemorrhage in the subcutaneous tissue	-0.04
Necrotic muscle fibers	0.02
Complement Factor D	0.02
Macrophages in the subcutaneous tissue	-0.01
Apolipoprotein A-I	0.004
Interferon Alpha 1	0.003
Neutrophils in the dermis	-0.0005

---

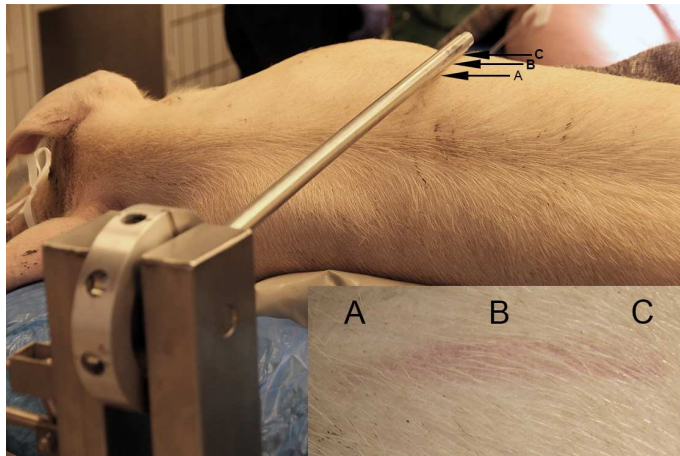
**Table 5:** The mean expression of 13 genes in the subcutaneous tissue of bruises aged 2, 5 and 8 h relative to the mean expression in uninjured subcutaneous fat tissue sampled from the thighs scaled to one. RE, relative expression; SEM, standard error of the mean.

	Control (n=12)		2 h (n = 4)		5 h (n = 4)		8 h (n = 4)	
Gene	RE	SEM	RE	SEM	RE	SEM	RE	SEM
APOA1	1.00	0.13	0.61	0.07	0.51	0.10	0.37	0.03
IL6	1.00	0.46	6.12	0.69	1.78	0.44	0.61	0.08
IFNA1	1.00	0.13	0.43	0.08	0.34	0.06	0.24	0.04
NFKB1	1.00	0.07	1.90	0.10	0.93	0.10	0.71	0.05
SELE	1.00	0.23	4.18	1.01	0.72	0.28	0.21	0.11
PTGS2	1.00	0.08	4.78	0.27	2.77	0.43	1.67	0.17
CFD	1.00	0.08	0.51	0.04	0.39	0.03	0.32	0.03
CCL2	1.00	0.18	7.59	0.89	6.66	1.56	2.81	0.54
ICAM1	1.00	0.16	3.72	0.70	0.85	0.17	0.60	0.07
FOS	1.00	0.39	3.73	0.49	1.85	0.48	1.08	0.18
PLAT	1.00	0.09	0.71	0.01	0.38	0.06	0.36	0.06
TNFAIP3	1.00	0.16	1.05	0.22	0.76	0.12	0.79	0.14
SELP	1.00	0.12	3.68	0.71	1.10	0.12	0.53	0.19

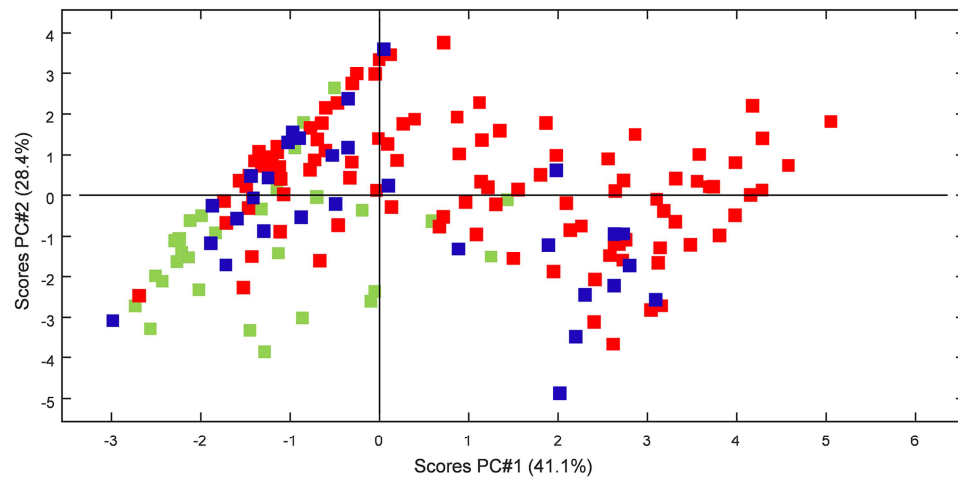


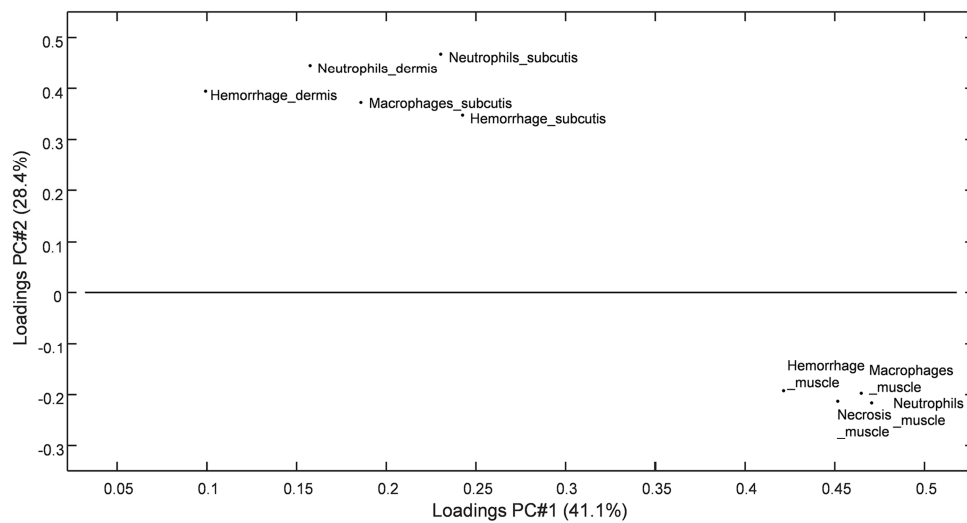


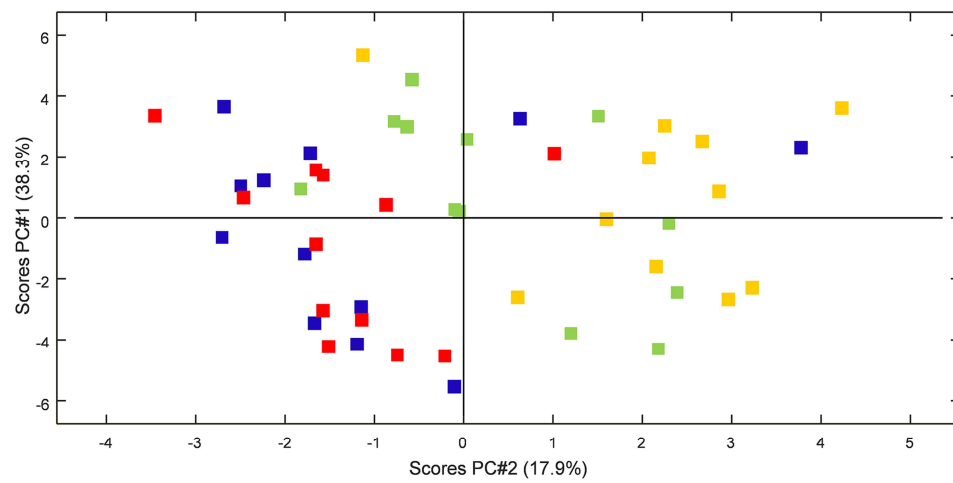


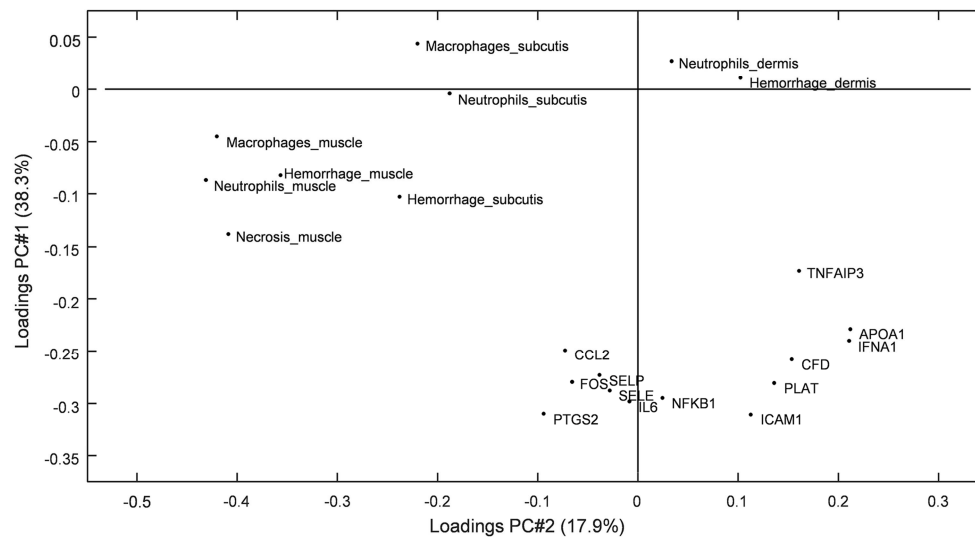


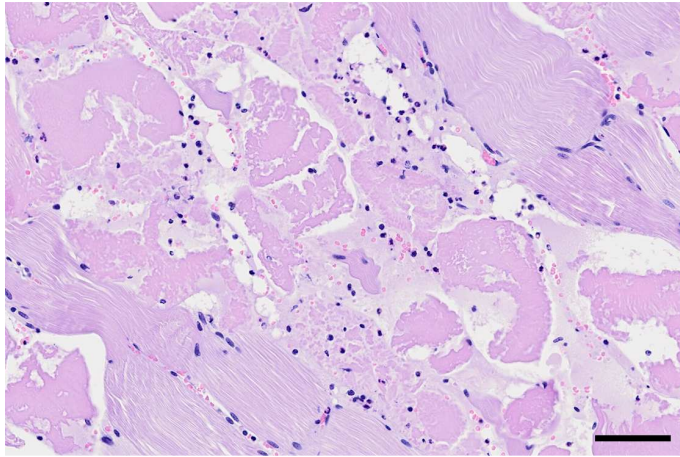


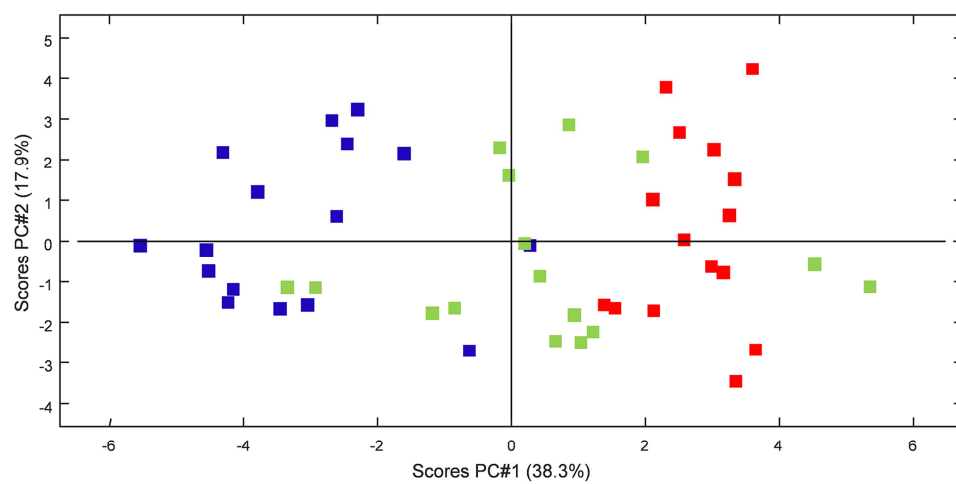


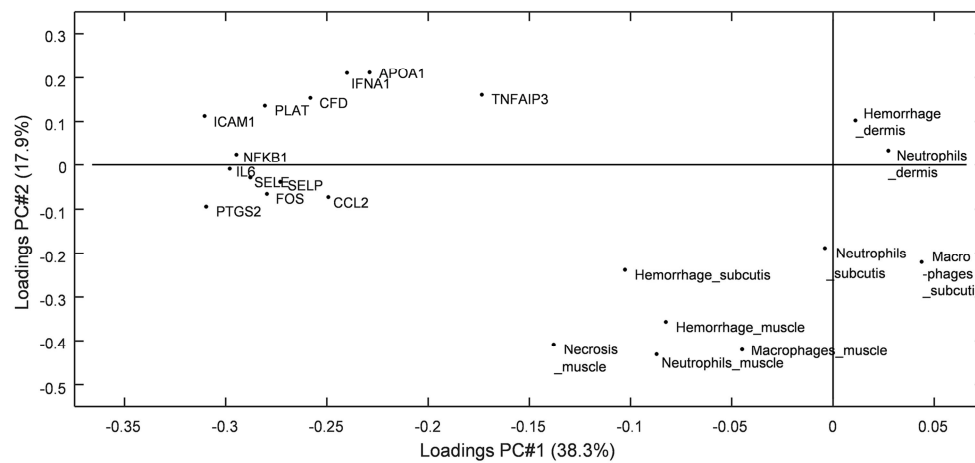












**Highlights**

- The inflammatory response was most pronounced in the center of the bruises.
- The intensity of inflammation in muscle depended on the thickness of the subcutis.
- Histology and mRNA expression data determined bruise age with a precision of  $\pm 2$ h.
- No difference was seen between bruises inflicted by a plastic tube and an iron bar.
- Experimental bruises were inflicted in 100kg slaughter pigs.